Polymer 50 (2009) 2664–2673

Contents lists available at ScienceDirect

Polymer

journal homepage: www.elsevier.com/locate/polymer

Influence of water and degree of sulfonation on the structure and dynamics of SPEEK studied by solid-state ^{13}C and ^{1}H NMR

Younkee Paik [a], Seen Ae Chae [a], Oc Hee Han [a,*], Sang Youp Hwang [b], Heung Yong Ha [b]

[a] Analysis Research Division, Daegu Center, Korea Basic Science Institute, 1370 Sankyuckdong, Bookgu, Daegu 702-701, Republic of Korea
[b] Fuel Cell Research Center, Korea Institute of Science and Technology, 39-1 Hawolgok-dong, Sungbuk-gu, Seoul 136-791, Republic of Korea

ARTICLE INFO

Article history:
Received 17 September 2008
Received in revised form
10 March 2009
Accepted 24 March 2009
Available online 7 April 2009

Keywords:
Sulfonated poly(ether-ether ketone) (SPEEK)
Solid-state nuclear magnetic resonance
Molecular motion

ABSTRACT

The molecular motions of sulfonated poly(ether-ether ketone) (SPEEK), synthesized by conventional method with a range of degree of sulfonation (DS) between 42 and 70%, as a function of DS and hydration were studied by ^{1}H-^{13}C dipolar recoupling by rotor-encoded longitudinal magnetization (RELM) and ^{13}C spin-lattice relaxations. The proton conductivity increased linearly with increasing DS from 52% and was comparable to that of Nafion 115 measured in the same condition for DS higher than 65%. The RELM dipolar patterns analyzed by the SIMPSON simulation program indicated that the population of phenyl rings in large amplitude motions such as 180°-flips was reduced with increasing DS. On the other hand, $T_{1\rho}$ (^{13}C) and T_1 (^{13}C) results suggested that the dynamic chains in both 66 kHz and 100 MHz regimes were more populated with increasing DS, possibly in small-amplitude oscillations.

1. Introduction

The polymer electrolyte membrane fuel cell (PEMFC) is a promising energy source for portable electronics, transportation, and large-scale stationary applications [1]. PEMFCs operate either on pure hydrogen or on hydrogen-rich compounds such as methanol [2]. The current choice of polymer membrane material for PEMFC is perfluorosulfonic polymers such as Nafion® [3]. However, the problems of Nafion membrane such as the high cost, low conductivity at low humidity or high temperature, and high methanol crossover have to be overcome to achieve successful commercialization.

Alternatively, novel hydrocarbon membrane materials have been investigated [4]. Sulfonated poly(ether-ether ketone) (SPEEK) exhibits good mechanical properties, high proton conductivity, and reduced permeability of methanol at low cost [5]. In addition, its properties can be optimized for fuel cell operating conditions by forming polymer blends or composites with various organic and/or inorganic compounds [6]. The proton conductivity of SPEEK-based materials depends primarily on the *degree of sulfonation* (DS), which represents the content of $-SO_3H$ per all possible $-SO_3H$ substitution sites. The DS can be determined by ^{1}H solution nuclear magnetic resonance (NMR) spectroscopy [7]. The $-SO_3H$ group causes a down field shift of the nearest neighboring proton (H_s) compared with the protons of the unsubstituted ether-ether phenyl ring (H_c and H_d) (Fig. 1). Since the numbers of the H_s and $-SO_3H$ groups are equivalent to each other, the DS is calculated from the peak area of H_s relative to the integral of the peak areas of all the other proton signals (H_x; x = a, b, c, d, a′, b′, c′, and d′) as follows:

$$\frac{\text{peak area}(H_s)}{\sum \text{peak area}(H_x)} = \frac{y}{12(1-y)+10y} = \frac{y}{(12-2y)};\quad (0 \le y \le 1)$$

where y represents the fraction of the repeat units substituted with an $-SO_3H$ group among all the repeat units in a polymer, as denoted in Fig. 1. Since the maximum number of $-SO_3H$ groups per repeat unit is one [8], DS (in %) = $y \times 100$. A high DS enhances the proton conductivity but reduces the mechanical and thermal stability of the polymer, with a balance between the two being found at a DS somewhere between 60 and 70% [7]. Material preparation conditions such as casting solvents and thermal history are also known to play important roles in determining the membrane properties and proton conductivity of SPEEK [9–11].

The molecular motions of poly(ether-ether ketone) (PEEK), the pristine material used for synthesizing SPEEK, have been the subject of many studies aiming to elucidate its good mechanical properties over a wide temperature range [12–14]. Correlations have been established between the chain motions of PEEK, such as cooperative phenyl-ring 180°-flips and segmental motions, and its mechanical behaviors [13]. However, to the best of our knowledge

* Corresponding author. Tel.: +82 53 950 7912; fax: +82 53 959 3405.
E-mail address: ohhan@kbsi.re.kr (O.H. Han).

0032-3861/$ – see front matter © 2009 Elsevier Ltd. All rights reserved.
doi:10.1016/j.polymer.2009.03.039

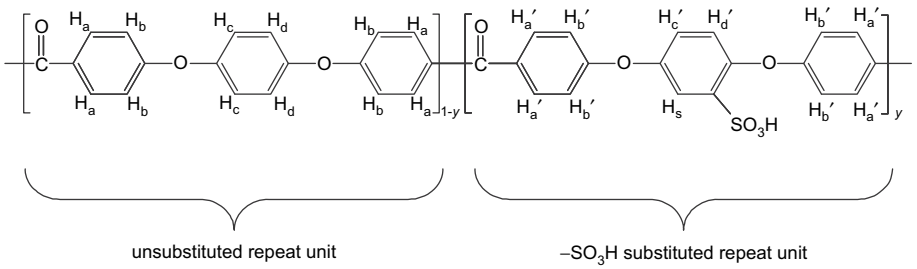

Fig. 1. Structure of the SPEEK repeat units and nomenclature of the aromatic protons.

no studies have yet been done on the correlations between the microscopic chain motions of SPEEK and DS and/or hydration.

Solid-state NMR spectroscopy has been successfully applied to characterize Nafion in various states [15–22]. The contents of water in and the methanol uptake of the membrane were determined quantitatively by ^{1}H NMR [17,23]. The glass transition of absorbed water in Nafion was detected by ^{1}H and ^{23}Na NMR [15,16]. The morphology and chain dynamics of the membrane as a function of water and/or methanol sorption have been characterized by solid-state ^{13}C, ^{19}F, and ^{129}Xe NMR [16,18,22]. Recently, a novel, water-channel model for the Nafion matrix, the so-called *inverted-micelle cylinder* model, was suggested based on small angle X-ray scattering (SAXS) and solid-state NMR data [24]. Narrower hydrophilic channels were observed in SPEEK, resulting in its low methanol crossover [5,21].

A series of ^{1}H-X heteronuclear recoupling experiments have been reported for studying the dynamics of the backbone and side chains of solid polymers, which are based on the simple rotational-echo double-resonance (REDOR) technique [25–28]. These methods may be characterized by the *rotor-encoding (RE)* period placed in the middle of the pulse sequences [27]. One of the main advantages of using these recoupling methods is that the size of the dipolar sideband patterns generated in the indirect dimension can be controlled by changing the length of the REDOR periods in the pulse sequence. Two different schemes are used depending on whether the actual density-operator evolutions start from the ^{1}H- or X-polarization: recoupled polarization-transfer and dipolar heteronuclear multi-spin correlation, respectively. The latter has an advantage in a system where X-nuclei are dipolar coupled to several ^{1}H spins [26]. Rotor-encoded longitudinal magnetization (RELM) is preferred to other heteronuclear dipolar recoupling methods when selective examination of a dipolar sideband pattern free from the effects of chemical shifts is required. However, most dipolar recoupling techniques require faster magic angle spinning (MAS) than 25 kHz by which the strong ^{1}H-^{1}H dipolar interactions are suppressed and spectral high resolution is achieved [29,30]. Recently, it was shown that RELM can be performed at a moderate sample spinning (below 10 kHz) with a larger rotor by implementing MREV-8 (Mansfield-Rhim-Elleman-Vaughan, 8 pulses per cycle) multiple pulses to ensure ^{1}H-^{1}H dipolar decoupling [31]. In this study, RELM, with this combination of a moderate spinning rate and MREV-8 multiple pulses, was used to improve the signal-to-noise ratios within a given experimental time.

In the present study, the chain motions of SPEEK, especially the nature and type of phenyl-ring motions, and the dynamics of water in SPEEK were studied as a function of hydration and DS by solid-state NMR techniques such as RELM, ^{1}H and ^{13}C spin-lattice relaxations. Spin-lattice relaxations in laboratory and rotating frames, T_1 and $T_{1\rho}$, respectively, are sensitive probes for molecular motions in different dynamical regimes: hundreds of MHz for T_1 and a few tens of kHz for $T_{1\rho}$ [32].

2. Experimental section

2.1. Synthesis of SPEEK and measurement of DS

Pristine PEEK material was purchased from Polysciences, Inc., USA. SPEEK was synthesized following the instructions in the literature [21]. Polymer of 20 g was dissolved in 500 mL of 98% sulfuric acid at room temperature and vigorously stirred. In the desired time interval, a portion of the sample was taken from the solution mixture and poured to a large excess of ice water under strong agitation. The polymer suspension was left to settle overnight. To remove any residual acid, the polymer precipitate was filtered and washed several times with distilled water until the pH was neutral (above 6.5). The polymer was then dried at room temperature for 2 days and then at 70 °C for another 2 days. A powder sample was prepared by grinding the dried polymer under liquid nitrogen. To measure DS, SPEEK solutions (3 wt.%) were prepared by dissolving the polymers in DMSO-d_6 with tetramethylsilane as an internal chemical shift standard and the ^{1}H solution NMR spectra of the solutions were taken on a Unity INOVA 500 MHz (Varian, U.S.A.) spectrometer.

2.2. Preparation of SPEEK membranes

SPEEK membranes were prepared by casting the 10 wt.% SPEEK solutions in dimethylacetamide onto a glass plate and drying at 70 °C overnight. To remove any residual solvents, the membranes were treated in 0.5 M H_2SO_4 solution at 70 °C for 3 h and rinsed with deionized water several times. The thickness of the resulting polymer membranes was in the range of 50–130 μm.

2.3. Proton conductivity measurements

The proton conductivity of the SPEEK membranes was measured by AC impedance spectroscopy over a frequency range of 10^2–10^6 Hz with an oscillating voltage of 5 mV using an IM6 Impedance Analyzer (Zahner, Germany). A membrane sample was clamped at the center of the cylindrical pathway of a test cell consisting of two compartments filled with 1 M H_2SO_4 solution [33,34]. Impedance data (R) across the membrane between the two Pt electrodes immersed in each compartment were recorded. The conductivity (σ) was calculated from the impedance data using the relation $\sigma = d/RA$, where d and A are the thickness and the face area of the membrane, respectively. The impedance of the solution only, for blank data, was measured without the membrane immediately before the measurements with the membrane. At least three runs were carried out for each measurement.

2.4. Water uptake of SPEEK membranes

To measure the uptake in water-saturated states, the membranes were first soaked in deionized water overnight at room

temperature and then weighed after the surface water was removed by Kimwipes. The membranes were then dried in an oven at 70 °C overnight and weighed again. The percentage weight gain with respect to the oven-dried membranes was taken as the water uptake of the water-saturated membranes. Partially hydrated SPEEK membranes were prepared by air-drying the water-saturated membranes on the bench until no weight gain or loss was noticeable within an hour. The percentage weight gain of these membranes with respect to their oven-dried membranes was taken as the water uptake of the partially hydrated membranes.

2.5. Solid-state NMR experiments

Solid-state NMR experiments were performed on an AVANCE II 400 MHz (Bruker, Germany) spectrometer using a double-resonance (H-X) MAS probe equipped with a 4-mm rotor. The resonance radio frequencies for ^{1}H and ^{13}C NMR were 400.1 and 100.6 MHz, respectively. The powder samples for solid-state NMR were prepared by grinding polymer films under liquid nitrogen. The sample rotor was spun at 9470 Hz. A pulse repetition delay of 2 s was used for all the NMR experiments in this work. A cross-polarization (CP) period of 1 ms was applied for all the experiments including a CP period. It was confirmed by ^{1}H NMR that the types and content of the absorbed water in the SPEEK samples did not change during the experimental times for solid-state NMR. Bisphenol A (4,4′-isopropyldienediphenol) and its polymer, polycarbonate (poly(bisphenol A carbonate)), powders were purchased from Sigma–Aldrich (U.S.A.) and used as standard samples for setting-up pulse sequences. Adamantane (Sigma–Aldrich, U.S.A.) was used as the external standard for referencing the solid-state ^{13}C (38.3 ppm for CH carbons) and ^{1}H (1.8 ppm) chemical shifts.

Fig. 2 shows the schematic of the pulse sequence for ^{1}H-^{13}C RELM experiments with MREV-8 homonuclear dipolar decoupling. The sequence consists of six parts: a preparation period for building up S-spin polarization, two REDOR dipolar recoupling periods, a wait period for removing unwanted antiphase coherence signals, a RE period in an indirect time dimension (t_1), and a detection time dimension (t_2) with TPPM decoupling. A detailed explanation of optimization and implementation of the pulse sequence was previously reported [31]. The 90° pulse length for both ^{1}H and ^{13}C was 2.2 μs. Four semi-windowless MREV-8 cycles, with a cycle period (t_c) of 26.5 μs, were used in each rotor period ($T_r = 106$ μs) for ^{1}H-^{1}H decoupling [35]. From the relationship of $t_c = 8 \times t_{dw}$, the dwell time (t_{dw}) for the RE dimension (t_1) was 3.3 μs. The maximum size of a window lacking ^{1}H-^{1}H decoupling during t_1 was less than 23.1 μs ($= 7 \times 3.3$ μs) [35]. Therefore, these experimental parameters were demonstrated to be practical for systems with homonuclear dipolar couplings less than about 30 kHz.

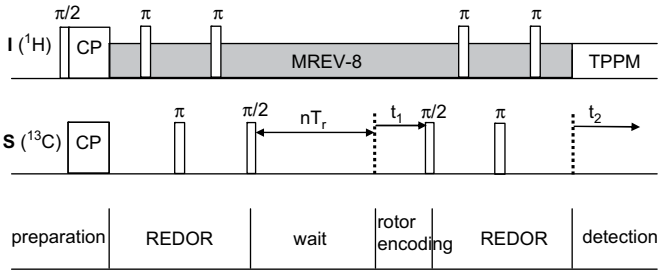

Fig. 2. Schematic representation of the pulse sequence for ^{1}H-^{13}C rotor-encoded longitudinal magnetization (RELM) experiments with MREV-8 homonuclear dipolar decoupling. The sequence consists of six parts: a preparation period for building up S-spin polarization, two REDOR dipolar recoupling periods, a wait period for removing unwanted antiphase coherence signals, a rotor-encoding period in an indirect time dimension (t_1) and a detection time dimension (t_2) with TPPM decoupling where n is the number of rotor cycles and T_r the rotor period.

Spin-lattice relaxation times of ^{13}C in a laboratory frame, T_1 (^{13}C)s, were measured using the T_{1CP} method by Torchia [36]. Spin-lattice relaxation times of ^{13}C in a rotating frame, $T_{1\rho}$ (^{13}C)s, were measured by varying the duration of the ^{13}C spin-locking pulse (at a nutation frequency of 66 kHz) applied after the CP period. T_1 (^{1}H) decay data were recorded with the inversion recovery pulse sequence [35]. Ninety degree pulse lengths of 2.7 and 3.8 μs for ^{13}C and ^{1}H, respectively, were used for single pulses while pulses at a nutation frequency of 66 kHz were applied for both ^{13}C and ^{1}H during CP.

3. Results and discussion

3.1. DS

The ^{1}H solution NMR spectra of SPEEK samples dissolved in DMSO-d_6 are shown in Fig. 3 and the peaks were assigned according to the literature [7]. At low sulfonation levels, most of the ^{1}H NMR peaks were broad and unresolved. This low spectral resolution was caused by the slower molecular motions of the polymer in solution resulting from the lower salvation of the polymer molecules at lower sulfonation levels. However, with increasing sulfonation levels, the peaks became narrow enough to be resolved. Using the peak areas, the DS values, listed in Table 1 along with the sample labels, were calculated as explained in the Introduction section. The DS values increased with increasing sulfonation time.

3.2. Proton conductivity

The conductivities of the SPEEK membranes are also listed in Table 1. The proton conductivity of the SPEEK membranes increased with increasing DS from 0.02 S/cm at DS = 42 to 0.11 S/cm at DS = 70. From DS = 52%, the conductivity increased almost linearly with increasing DS and became comparable to the conductivity (0.10 S/cm) of Nafion 115 measured in the same condition for DS

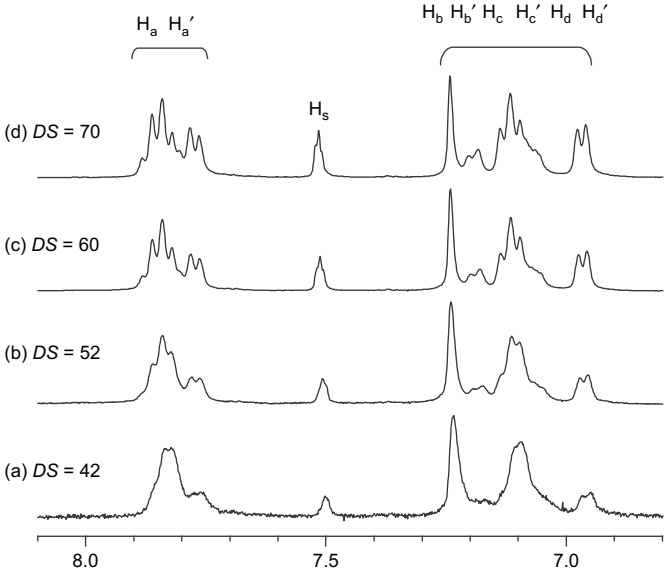

Fig. 3. Solution-state ^{1}H NMR spectra of SPEEK samples (3 wt.% in DMSO-d_6) on increasing the degree of sulfonation (DS) (refer to Fig. 1 for proton designation and text for the definition of DS).

Table 1
Degree of sulfonation (DS) and proton conductivity of the SPEEK membranes.

Sample	Sulfonation time (h)	DS[a] (%)	Proton conductivity[b] (S/cm)
SPEEK-42	96	42	0.020
SPEEK-52	168	52	0.022
SPEEK-56	216	56	0.032
SPEEK-60	288	60	0.063
SPEEK-62	360	62	0.067
SPEEK-70	408	70	0.11

[a] DS, refer to the text for the definition, was measured by solution-state ^{1}H NMR.
[b] Proton conductivity was measured in 1 M H_2SO_4 solution.

higher than 65% (Fig. 4). The measured conductivities were consistent with those provided in the literature [5,34].

3.3. Water uptake

Table 2 shows the water content of the SPEEK membranes versus the DS and hydration level. The water uptake of the membranes increased with increasing DS [7,37]. In water-saturated membranes, the average number of water molecules per $-SO_3H$ group (n) also increased with increasing DS. On the other hand, the partially hydrated samples contained the same number of water molecules per $-SO_3H$ group.

3.4. Solid-state ^{1}H MAS and ^{13}C CP MAS NMR spectra

Fig. 5 shows the ^{1}H MAS NMR spectra of PEEK and SPEEKs acquired at a sample spinning of 9.47 kHz. The phenyl protons of PEEK gave rise to a broad resonance at 6.4 ppm. Upon sulfonation, the spectra gave rise to an additional resonance at 8.5 ± 0.3 ppm for the absorbed water and sulfonic proton in the partially hydrated samples (Fig. 5b–e). The high chemical shift (8.5 ppm) of absorbed water compared with bulk water (4.8 ppm) reflected the strongly acidic environment around the $-SO_3H$ groups when n is about 4. On the other hand, as n increased, the ^{1}H chemical shift decreased, as shown with the water-saturated samples (Fig. 5f–h). Therefore, as in the case of Nafion [17], the ^{1}H chemical shift may be used as a sensitive measure of the water content of SPEEKs.

Fig. 6 shows the solid-state ^{13}C CP MAS NMR spectra of PEEK and SPEEK-70. The ^{13}C NMR spectra of SPEEK-70 were very similar to the spectrum of PEEK, except that a relatively small component was hidden under the shoulder of the C-1 peak at 137 ppm (Fig. 6). The substitution of an $-SO_3H$ group caused a down field shift of C-5_a by 15 ppm compared with the unsubstituted ones (C-5 at 122 ppm). No significant difference was observed between the two spectra of SPEEK-70 membranes with different water contents (Fig. 6b and c), except that the spectral intensity of the water-saturated sample (Fig. 6c) was only one-fifth of that of the partially hydrated sample (Fig. 6b), even though the scan number for the former at the reoptimized CP conditions for longer 90° pulse lengths was twice that of the latter. This was due to the lowered Q factor of the coil for wet samples, as reported in the literature [38]. Neither decreasing CP times from 1.0 to 0.1 ms nor increasing the experimental temperature up to 85 °C greatly improved the spectral intensities, indicating that the primary cause of the signal loss was *not* the chain segmental motions in intermediate regimes. The solid-state ^{13}C CP MAS NMR spectra of other SPEEK-X (X = 42, 50, 60) samples were almost identical to those of SPEEK-70 and the spectral resolution of ^{13}C NMR for the SPEEKs was, in general, very poor in part due to the molecular structure and ordering heterogeneities [32].

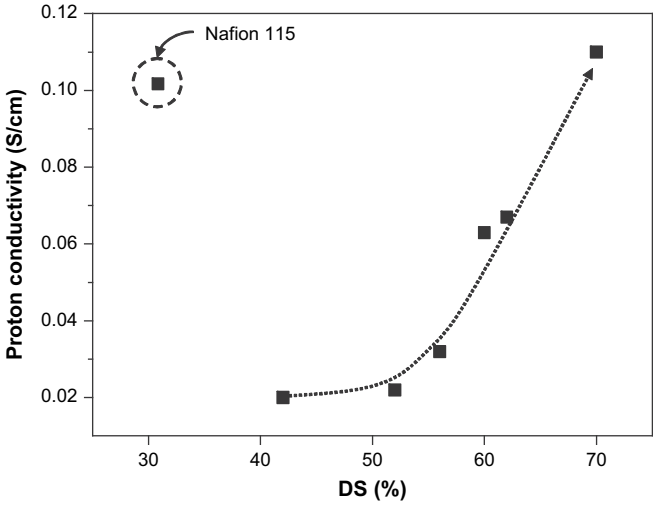

Fig. 4. Proton conductivity of the SPEEK membranes as a function of the degree of sulfonation (DS), measured in 1 M H_2SO_4 solution. The proton conductivity of Nafion 115 measured at the same condition is placed in the plot for comparison and the dotted line with an arrow at the upper end is provided as a guide.

The characterization of the chain dynamics of SPEEK by ^{13}C NMR is complicated due to the compactness of the spectral lines in the aromatic-carbon region. The signal at 132 ppm arose from both the protonated and non-protonated carbons of the ether-ether phenyl rings (C-1). The broad peak near 120 ppm can be deconvoluted into two spectral components [12]: one centered at 122 ppm for the C-5 carbons of the ether-ether phenyl rings and the other centered at 117 ppm for the C-2 carbons of the ether-ketone phenyl rings. Therefore, the signal at 122 ppm was attributed to all the protonated carbons of the ether-ether phenyl rings, both with and without $-SO_3H$ groups. On the other hand, the resonance at 117 ppm arose only from the ether-ketone phenyl rings not substituted with any $-SO_3H$ groups. Therefore, the spectral line at 117 ppm for C-2 was chosen for the quantitative analyses of the chain dynamics of SPEEK and sulfonation effects as below.

3.5. Chain dynamics studied by T_1 (^{13}C) and $T_{1\rho}$ (^{13}C) of C-2

The semilog plots of the T_1 (^{13}C) decay data of the C-2 carbons in PEEK and water-saturated SPEEK-X (X = 52, 60, 70) are shown in Fig. 7a. The curvatures in the signal decays represent the heterogeneous nature of the chain dynamics involving the C-2 carbons [32] The T_1 (^{13}C) values of the C-2 carbons of the samples were obtained from the initial slopes of the curved decays and are listed in Table 3. As the DS increased from 52% (SPEE-52) to 70% (SPEEK-70), the T_1 (^{13}C) values decreased gradually from 11 to 5.1 s, thereby implying an increase of chain mobility. The water content also influenced the T_1 (^{13}C) decay data of the C-2 carbons, as demonstrated with the water-saturated (35 wt.%) and partially hydrated (10 wt.%) SPEEK-70 in Fig. 7b.

Table 2
The water content and ^{1}H spin-lattice relaxation times of absorbed water in the SPEEK membranes.

Sample	Partially hydrated			Water-saturated		
	Water uptake (wt.%)	n[a]	T_1 (^{1}H)[b] (s)	Water uptake (wt. %)	n[a]	T_1 (^{1}H)[b] (s)
PEEK	0	0	1.7[c]	0	0	N/A
SPEEK-52	8	4	0.21	20	8	0.04
SPEEK-60	9	4	0.13	30	11	0.04
SPEEK-70	10	4	0.04	35	12	0.03

[a] $n = [H_2O/SO_3H]$.
[b] Obtained from the least-squares-straight-line fit of the observed decay data between 0.01 and 30 ms in Fig. 11.
[c] This value is for the phenyl-ring protons.

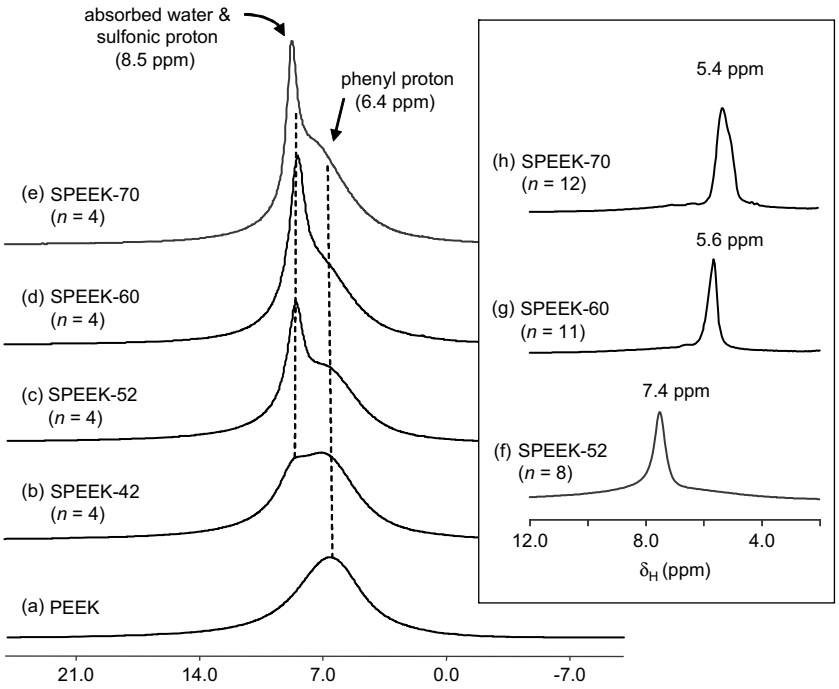

Fig. 5. Solid-state ^{1}H MAS NMR spectra of: (a) PEEK, (b)–(e) partially hydrated SPEEK-X and (f)–(h) water-saturated SPEEK-X samples where *X* is the degree of sulfonation (DS). The number of water molecules per $-SO_3H$ group (*n*) is indicated on the spectrum (refer to Table 2 for water in wt.%). The samples were spun at 9.47 kHz.

The semilog plots of the $T_{1\rho}$ (^{13}C) decay data of the C-2 carbons of PEEK and water-saturated SPEEK-X (X = 52, 60, 70) are shown in Fig. 8a. The $T_{1\rho}$ (^{13}C) values of the C-2 carbons of water-saturated SPEEK-X, calculated from the initial slopes and given in Table 3, were similar to one another with increasing DS, in contrast to the dramatically varied T_1 (^{13}C) values. The semilog plots of the $T_{1\rho}$ (^{13}C) decay data of the C-2 carbons of the water-saturated (35 wt.%) and partially hydrated (10 wt.%) SPEEK-70 are compared in Fig. 8b. The

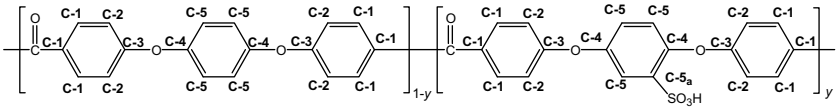

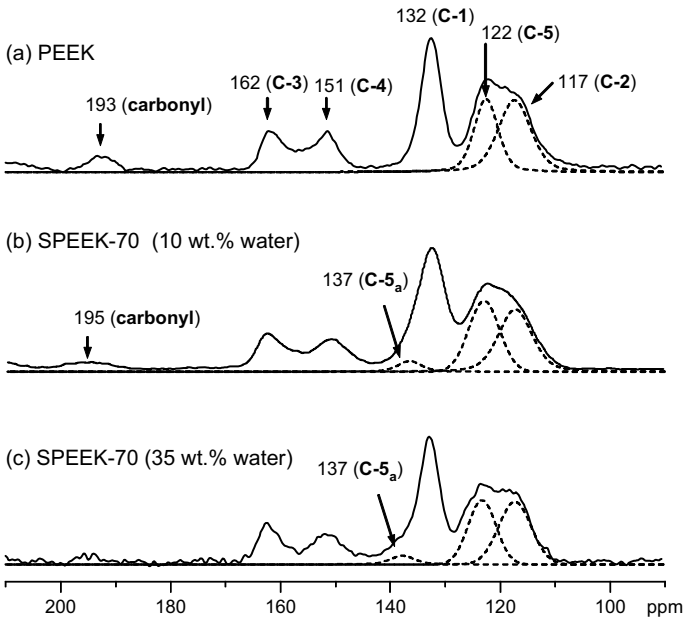

Fig. 6. Solid-state ^{13}C CP MAS NMR spectra of: (a) PEEK and (b)–(c) SEEK-70 at different water uptakes. The carbon designation for the repeat units of SPEEK-70 is given at the top and C-5_a is replaced with C-5 for PEEK since the $-SO_3H$ group is replaced with H.

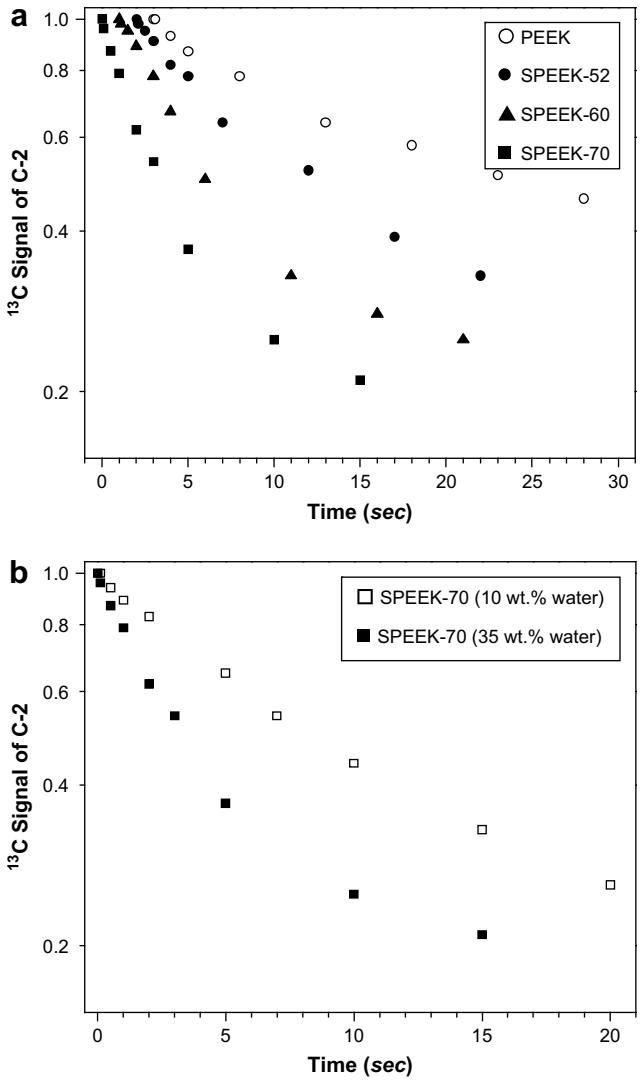

Fig. 7. Semilog plots of the ^{13}C spin-lattice relaxation (T_1 (^{13}C) at 100 MHz) decay data of the C-2 carbons of ether-ketone phenyl rings in PEEK and SPEEK-X where *X* is the degree of sulfonation (DS): (a) as a function of DS for water-saturated SPEEK samples and PEEK, and (b) SPEEK-70 at different water uptakes. The plots in (a) have been displaced by 1 s in the horizontal direction from one another for clarity.

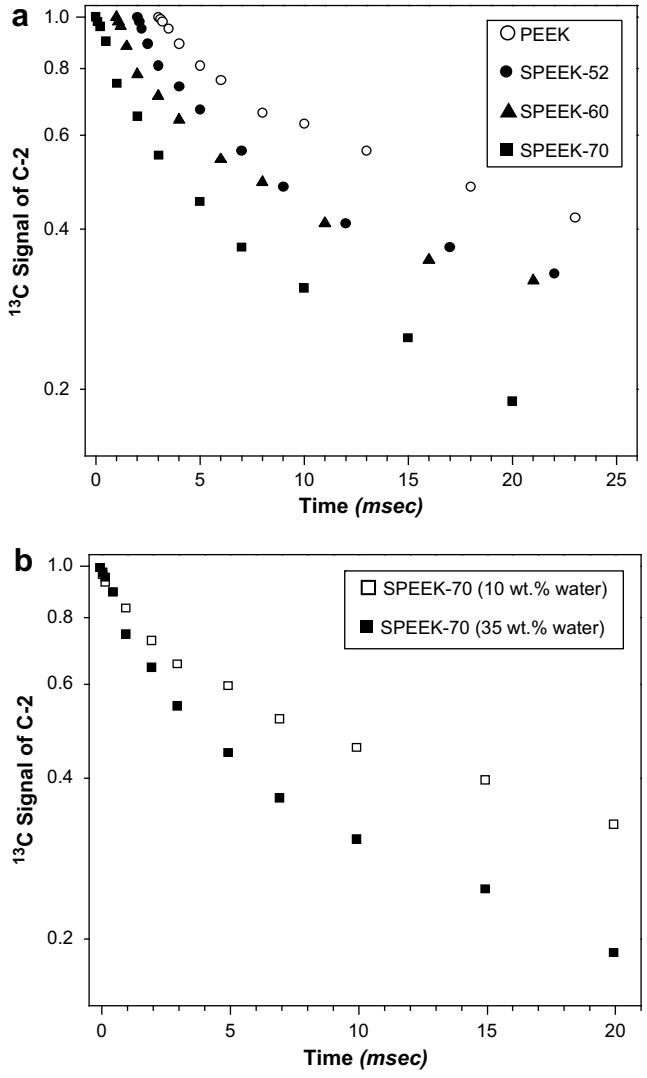

Fig. 8. Semilog plots of the ^{13}C spin-lattice relaxation decay data in the rotating frame ($T_{1\rho}$ (^{13}C) at 60 kHz) of the C-2 carbons of ether-ketone phenyl rings in PEEK and SPEEK-X where X is the degree of sulfonation (DS): (a) as a function of DS for water-saturated SPEEK samples and PEEK, and (b) SPEEK-70 at different water uptakes (wt.%). The plots in (a) have been displaced by 1 ms in the horizontal direction from one another for clarity.

initial slope difference between the two plots was less pronounced compared with that found in the corresponding T_1 (^{13}C) decay data in Fig. 7b. The above results suggested that the chain dynamics of SPEEK increased with increasing DS and as a function of both DS and water content. The more pronounced dependence of T_1 (^{13}C), compared to $T_{1\rho}$ (^{13}C), on the water content indicates that the molecular motions in the ~100 MHz regime were more affected by water content than those in the ~66 kHz regime.

Table 3
^{13}C spin-lattice relaxation times of PEEK and SPEEK-X where *X* is the degree of sulfonation (DS).

Sample	Partially hydrated[a]		Water-saturated[b]	
	T_1 (^{13}C)[c] (s)	$T_{1\rho}$ (^{13}C)[d] (ms)	T_1 (^{13}C)[c] (s)	$T_{1\rho}$ (^{13}C)[d] (ms)
PEEK	20	9.3	N/A	N/A
SPEEK-52	12	6.6	11	5.7
SPEEK-60	11	6.6	7.1	5.6
SPEEK-70	11	6.3	5.1	4.5

[a] Refer to Table 2 for the water content of each sample from $n = [H_2O/SO_3H]$.
[b] Refer to Table 2 for the water content of each sample from the least-squares-straight-line fit of the observed decay data between 0.01 and 30 ms in Fig. 11.
[c] From the least-squares-straight-line fit of the observed decay data between 0.01 and 3 s in Fig. 7.
[d] From the least-squares-straight-line fit of the observed decay data between 0.01 and 2 ms in Fig. 8.

3.6. Chain dynamics studied by ^{1}H-^{13}C RELM

The RELM experiments were performed on the partially hydrated samples, rather than the water-saturated one, since the ^{1}H nutation frequencies of the water-saturated samples of SPEEK-X (X = 52, 60, 70) were too long for the RELM experiments. The representative ^{1}H-^{13}C RELM spectra of the partially hydrated SPEEK-70 are shown in Fig. 9, in which only the signals for the C-1, C-2, and C-5 carbons have modulations in the spectral intensity along the dipolar (t_1) dimension. However, one-third of the C-1 carbons were quaternary carbons, while all the C-2 and C-5 carbons were protonated so that the peak-modulation of the C-1 carbons at 132 ppm was not complete. The signal evolution plot of the C-2

carbons along the t_1 axis and its dipolar spectrum is shown in Fig. 9b and c, respectively. All the odd-numbered dipolar sidebands disappear in the RELM experiments [39]. The span of the dipolar spectrum is very sensitive to the phenyl rings undergoing 180°-flips with frequencies comparable to or greater than the dipolar coupling of about 10 kHz [31,32,39,40].

The experimental dipolar sideband patterns, represented as solid bars, for the static phenyl rings of bisphenol A (Fig. 10a) and the phenyl rings of polycarbonate [41] flipping faster than 10 kHz (Fig. 10b) were clearly distinguishable from each other. The experimental dipolar sideband patterns were fit to the calculated dipolar sideband patterns, represented as open bars, using the SIMPSON program [42] with ^{1}H-^{13}C dipolar coupling constants of 10.5 and 6.5 kHz, respectively. The dipolar sideband pattern of bisphenol A induced an averaged MREV-8 scale factor of 0.45. A motional scale factor ($f = D_{\mathrm{eff}}/D_{\mathrm{static}}$) was used to denote the degree of reduction of the dipolar coupling constant due to molecular motions [32] where D_{eff} is the effective dipolar coupling constant of an isolated ^{1}H-^{13}C spin pair in molecular motions and D_{static} is that for a static ^{1}H-^{13}C spin pair. A motional scale factor of 0.62 with $D_{\mathrm{eff}} = 6.5$ kHz was obtained for the dipolar sideband pattern of polycarbonate (Fig. 10(b)), which is consistent with the theoretical f value (0.625) calculated for a ^{1}H-^{13}C pair in the ortho (or meta)-position of a phenyl ring undergoing 180°-flips along its C1–C4 axis [32]. The dipolar sideband pattern of PEEK (Fig. 10(c)) induced a D_{eff} of 8.5 kHz, resulting in an f value of 0.81, while the dipolar sideband pattern of the partially hydrated SPEEK-70 with 10 wt.% water (Fig. 10(d)) induced a D_{eff} of 10.0 kHz and an f value of 0.95. The intensities of the dipolar sidebands, D_{eff}, and f for all SPEEK-X (X = 42, 52, 60, 70) are listed in Table 4. The D_{eff} for the ether-ketone phenyl rings in SPEEK-X (X = 42, 52, 60, 70) increased with increasing DS. It has been reported that 10–20% of the ether-ketone phenyl rings of PEEK undergo 180°-flips at room temperature [12,39]. When the heterogeneous motions of the phenyl rings observed in PEEK are considered, the experimental dipolar sideband pattern of PEEK was better simulated by assuming that about 40% of the ether-ketone phenyl rings additionally undergo 180°-flips, as shown in Fig. 10(e). The remaining ether-ketone phenyl rings were assumed to be in the same heterogeneous motional state with the ether-ketone phenyl rings of bisphenol A. Likewise, the dipolar sideband pattern of SPEEK-70 was better fitted, as demonstrated in Fig. 10(f), when an additional 15% of the ether-ketone phenyl rings were in 180°-flip motions. These results suggest that sulfonation reduces the population of the ether-ketone phenyl rings in 180°-flip motions.

Thermodynamic studies on Nafion have shown that absorbed water causes a hydraulic pressure of about 300–600 bars in the polymer matrix [43,44]. It is likely that this internal pressure from the absorbed water suppresses the flipping of the ether-ketone phenyl rings at room temperature. Thus the decreased T_1 (^{13}C) and

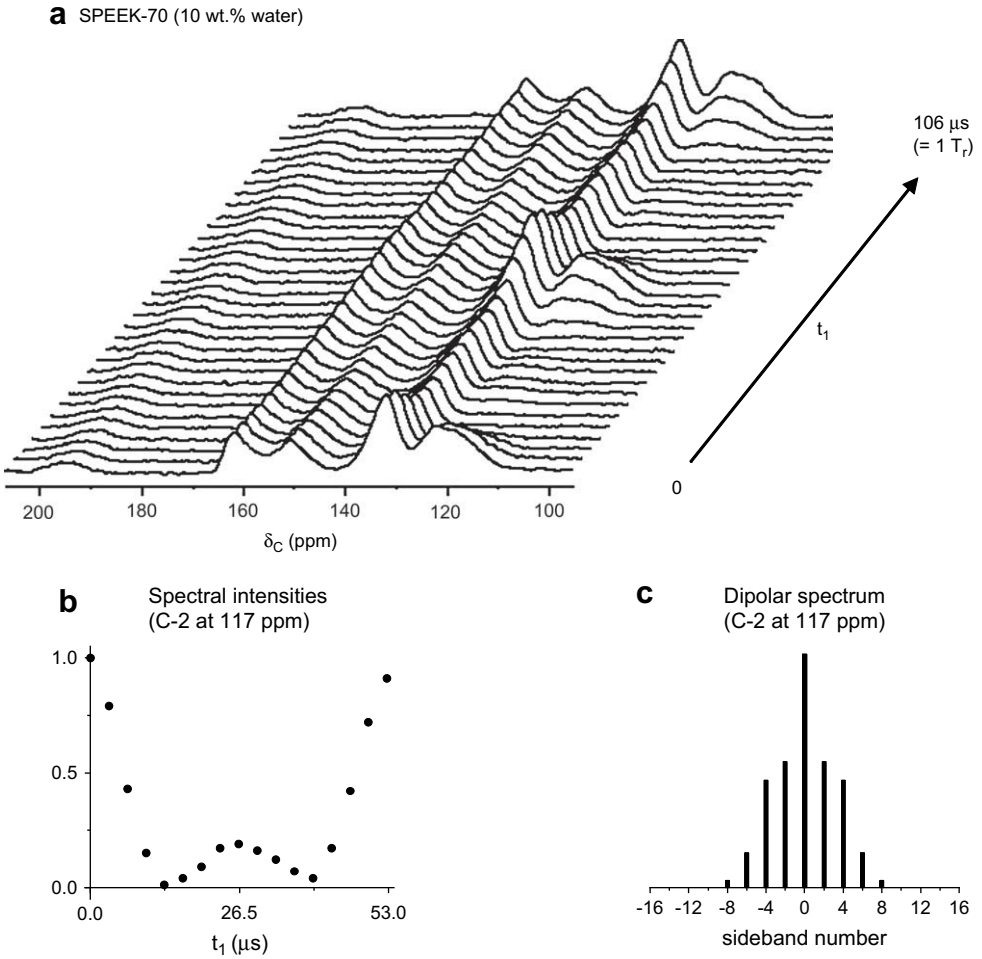

Fig. 9. (a) ^{1}H-^{13}C RELM spectra of partially hydrated SPEEK-70 with 10 wt.% water acquired with MREV-8 multiple pulses and a sample spinning at 9.47 kHz for one rotor period ($1T_r$) (see Fig. 6 for peak assignments). (b) Evolution of the spectral intensities of the C-2 carbons at 117 ppm; for clarity only a half rotor period is shown. (c) ^{1}H-^{13}C dipolar spectrum obtained by 32-discrete Fourier transform of the time-domain signals shown in (b).

$T_{1\rho}$ (^{13}C) values (see above) may be due to enhanced, small amplitude, phenyl ring oscillations, as suggested on PEEK [13], rather than phenyl ring flips. Similar phenomena have been reported for hydration-induced, enhanced oscillations of side chains and backbones of Nafion [43,44].

3.7. Water dynamics studied by T_1 (^{1}H)

The semilog plots of T_1 (^{1}H) decay data for water absorbed in SPEEK are shown in Fig. 11. The T_1 (^{1}H) values calculated from the initial slopes of the decays are listed in Table 2. The T_1 (^{1}H) values of the partially hydrated SPEEK samples decreased drastically from 0.21 s for SPEEK-52 to 0.04 s for SPEEK-70, although n in the partially hydrated samples was the same as 4 (Table 2). Therefore, the observed decrease in T_1 (^{1}H) should be correlated with the water dynamics induced by the degree of formation of water channels rather than by the size variation of each $-SO_3H$ group clustered with water molecules. A recent study showed that ion pairing between $-SO_3^-$ groups occurred when n is higher than 2, with hydrogen-bonded network developing for $n \geq 3$, in a 73% sulfonated SPEEK [21]. The DS of all the SPEEK samples investigated in the present study was lower than 73%, supporting the plausibility that the ion pairing and/or water-channel of SPEEK-X ($X \leq 70$) starts to form at different n depending on DS, and requires n to be 4

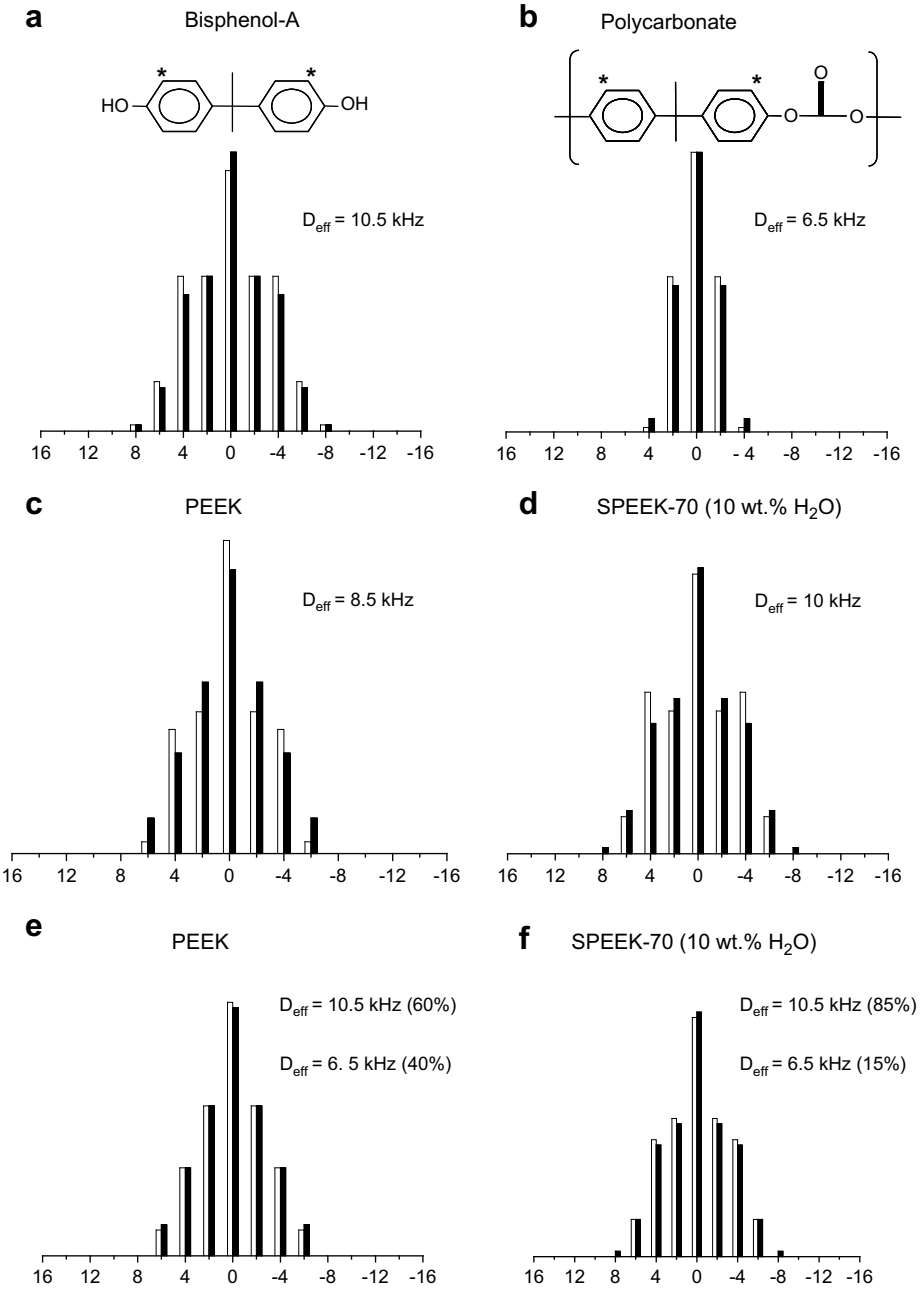

Fig. 10. Comparison of the experimental (solid bars) and simulated (open bars) ^{1}H-^{13}C RELM dipolar sideband patterns of: the protonated phenyl-ring carbons (*) of bisphenol A (a) and polycarbonate (b), and the C-2 carbons of the ether-ketone phenyl rings in PEEK [(c) and (e)] and in partially hydrated SPEEK-70 with 10 wt.% water [(d) and (f)]. The effective dipolar coupling constant (D_{eff}) used for the simulations is marked on individual patterns. The simulated patterns in (e) and (f) were obtained by combining two different D_{eff} values of 10.5 and 6.5 kHz together. They were then compared with the counter parts in (c) and (d) obtained with single D_{eff} values.

Table 4
^{1}H-^{13}C RELM dipolar sideband intensities obtained experimentally, and effective dipolar coupling constants and motional scale factors obtained by simulation.

Sample	Sideband number[a]					D_{eff}[d] (kHz)	f[e]
	0	2	4	6	8		
Bisphenol A[b]	0.45	0.25	0.22	0.07	0.01	10.5	1.0
Polycarbonate[b]	0.63	0.33	0.03	–	–	6.5	0.62
PEEK[c]	0.48	0.29	0.17	0.06	–	8.5	0.81
SPEEK-42[c]	0.45	0.27	0.20	0.07	0.01	9.0	0.90
SPEEK-52[c]	0.44	0.27	0.20	0.07	0.02	9.5	0.91
SPEEK-60[c]	0.44	0.26	0.21	0.07	0.01	10.0	0.95
SPEEK-70[c]	0.46	0.25	0.21	0.07	0.01	10.0	0.95

[a] The intensities of the odd-numbered sidebands were omitted as they were all zero.
[b] For all the protonated phenyl carbons.
[c] For the C-2 carbons of the ether-ketone phenyl rings in partially hydrated samples (Refer to Table 2 for the water contents).
[d] Effective dipolar coupling constant obtained by the simulation using the SIMPSON program.
[e] Motional scale factor (see text for the definition) obtained by the simulation using the SIMPSON program.

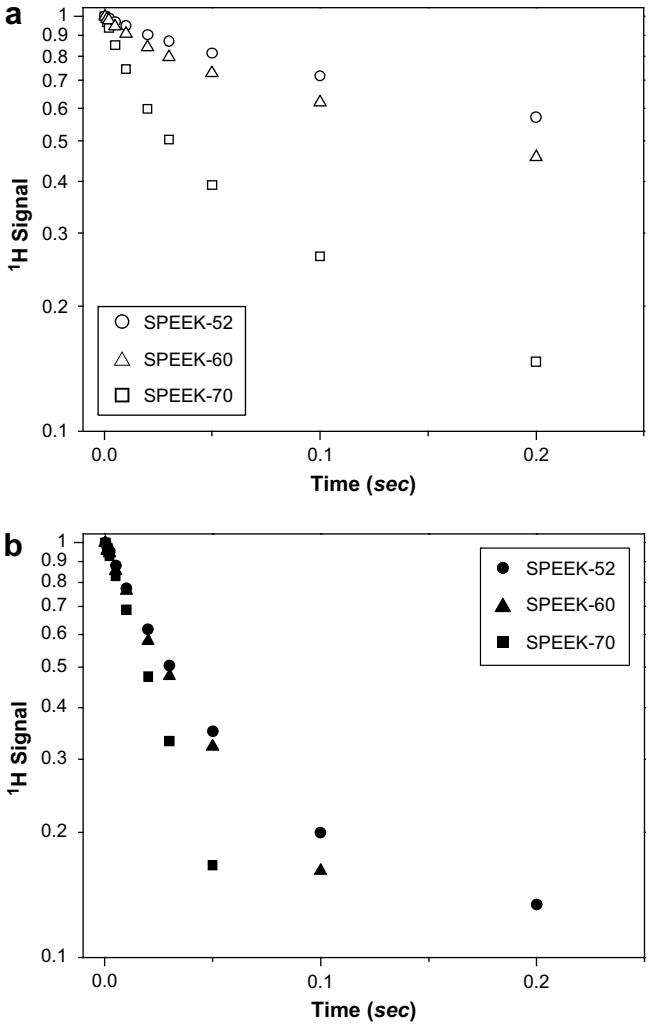

Fig. 11. Semilog plots of the ^{1}H spin-lattice relaxation (T_1 (^{1}H) at 400 MHz) decay data of the absorbed water and sulfonic proton in SPEEK-X as a function of degree of sulfonation (DS) where X is DS: for (a) partially hydrated samples and (b) water-saturated samples. Refer to Table 2 for the water contents.

or more for full formation. The T_1 (^{1}H) values of the water-saturated SPEEK samples of $n \geq 8$ and partially hydrated SPEEK-70 were almost identical, regardless of the DS, indicating that water channels might have already been fully developed. The T_1 (^{1}H) values of the water-saturated samples were, in general, shorter than those of the partially hydrated samples (Table 2).

4. Conclusions

The SPEEK membranes were prepared in a range of DS between 42 and 70%. The proton conductivity of the membranes increased with increasing DS almost linearly from 52%. The ^{1}H-^{13}C RELM results on the partially hydrated samples indicated that the 180°-flip motions of the ether-ketone phenyl rings, to which $-SO_3H$ groups do not attach directly, in SPEEK were reduced compared with those in PEEK at room temperature. On the contrary, both T_1 (^{13}C) and $T_{1\rho}$ (^{13}C), which reflect small-amplitude motions in approximately 100 MHz and 66 kHz regimes, respectively, decreased with increasing DS of water-saturated SPEEK, indicating an increase of small-amplitude oscillations. The oscillations in the ~100 MHz regime were more drastically enhanced in a greater hydration state. The T_1 (^{1}H) values of absorbed water decreased drastically with increasing DS in the partially hydrated SPEEK samples. This was ascribed to the changes in water dynamics associated with water-channel formation in SPEEK: the n required for the start of water-channel formation varied according to DS and was 4 or more for full formation. In contrast, the T_1 (^{1}H) values of absorbed water in the water-saturated SPEEK samples were nearly identical among the samples but were much smaller than those of partially hydrated SPEEK samples, implying the complete development of water channels in the water-saturated SPEEK samples. Our T_1 (^{1}H) data also suggest that SPEEK has water channels in much smaller sizes than Nafion. The proton conductivity increased linearly with increasing DS from 52% and was comparable to that of Nafion 115 measured in the same condition for DS higher than 65%. Therefore, our study results have demonstrated that increasing the DS not only influences the proton conductivity but also induces changes in the molecular motions of SPEEK chains by increasing the water uptake.

Acknowledgment

This work was supported by the Korea Research Council of Fundamental Science and Technology through the STRM program (grant number: C-Research-07-04-KBSI).

References

[1] Carrette L, Friedrich KA, Stimming U. Fuel Cells 2001;1:5–39.
[2] Arico AS, Srinivasan S, Antonucci V. Fuel Cells 2001;1:133–61.
[3] Mauritz KA, Moore RB. Chem Rev 2004;104:4535–85.
[4] Hickner MA, Ghassemi H, Kim YS, Einsla BR, McGrath JE. Chem Rev 2004;104:4587–612.
[5] Kreuer KD. J Membr Sci 2001;185:29–39.
[6] Zhang H, Li X, Zhao C, Fu T, Shi Y, Na H. J Membr Sci 2008;308:66–74.
[7] Zaidi SMJ, Mikhailenko SD, Robertson GP, Guiver MD, Kaliaguine S. J Membr Sci 2000;173:17–34.
[8] Xing P, Robertson GP, Guiver MD, Mikhailenko SD, Wang K, Kaliaguine S. J Membr Sci 2004;229:95–106.
[9] Robertson GP, Mikhailenko SD, Wang K, Xing P, Guiver MD, Kaliaguine S. J Membr Sci 2003;219:113–21.
[10] Reyna-Valencia A, Kaliaguine S, Bousmina M. J Appl Polym Sci 2005;98:2380–93.
[11] Reyna-Valencia A, Kaliaguine S, Bousmina M. J Appl Polym Sci 2006;99:756–74.
[12] Poliks MD, Schaefer J. Macromolecules 1990;23:3426–31.
[13] Chen CL, Lee CL, Shih JH. Macromolecules 1994;27:7872–6.
[14] Clayden NJ. Polymer 2000;41:1167–74.
[15] Komoroski RA, Mauritz KA. J Am Chem Soc 1978;100:7487–9.
[16] Boyle NG, McBrierty VJ, Eisenberg A. Macromolecules 1983;16:80–4.
[17] Bunce NJ, Sondheimer SJ, Fyfe CA. Macromolecules 1986;19:333–9.

[18] Meresi G, Wang Y, Bandis A, Inglefield PT, Jones AA, Wen WY. Polymer 2001;42:6153–60.
[19] Liu S-F, Schmidt-Rohr K. Macromolecules 2001;34:8416–8.
[20] Chen Q, Schmidt-Rohr K. Macromolecules 2004;37:5995–6003.
[21] Ye G, Janzen N, Goward GR. Macromolecules 2006;39:3283–90.
[22] Chen Q, Schmidt-Rohr K. Macromol Chem Phys 2007;208:2189–203.
[23] Skou E, Kauranen P, Hentschel J. Solid State Ionics 1997;97:333–7.
[24] Schmidt-Rohr K, Chen Q. Nat Mater 2007;7:75–83.
[25] Gullion T, Schaefer J. Macromolecules 1989;81:196–200.
[26] Saalwachter K, Spiess HW. J Chem Phys 2001;114:5707–28.
[27] Saalwachter K, Schnell I. Solid State Nucl Magn Reson 2002;22:154–87.
[28] Rapp A, Schnell I, Sebastiani D, Brown SP, Percec V, Spiess HW. J Am Chem Soc 2003;125:13284–97.
[29] Brown SP, Spiess HW. Chem Rev 2001;101:4125–55.
[30] Schnell I, Spiess HW. J Magn Reson 2001;151:153–227.
[31] Paik Y, Poliks B, Rusa CC, Schaefer J. J Polym Sci Part B Polym Phys 2007;45:1271–82.
[32] Schaefer J, Stejskal EO, McKay RA, Dixon WT. Macromolecules 1984;17:1479–89.
[33] Cappadonia M, Erning JW, Stimming U. J Electroanal Chem 1994:189.
[34] Gil M, Ji X, Li X, Na H, Hampsey JE, Lu Y. J Membr Sci 2004;234:75–81.
[35] Carr HY. Phys Rev 1954;94:630–8.
[36] Torchia DA. J Magn Reson 1969;30:613–6.
[37] Li L, Zhang J, Wang Y. J Membr Sci 2003;226:159–67.
[38] Stringer JA, Bronnimann CE, Mullen CG, Zhou DH, Stellfox SA, Li Y, et al. J Magn Reson 2005;173:40–8.
[39] De Paul SM, Saalwachter K, Graf R, Spiess HW. J Magn Reson 2000;146:140–56.
[40] Munowitz MG, Griffin RG. J Chem Phys 1982;76:2848–58.
[41] Schaefer J, McKay RA, Stejskal EO. J Magn Reson 1983;52:123–9.
[42] Bak M, Rasmussen JT, Nielsen NC. J Magn Reson 2000;147:296–330.
[43] Escoubes M, Pineri M, Robens E. Thermochim Acta 1984;1:149–60.
[44] Hsu WY, Gierke TD. Macromolecules 1982;15:101–5.